

# Exploring DSNB boosted sub-GeV dark matter: insights from XENONnT and LZ experiments

PPC 2024

17th International Conference on Interconnections between Particle Physics and Cosmology

**Anirban Majumdar**

Indian Institute of Science Education and Research - Bhopal

(In collaboration with V. D. Romeri, D. K. Papoulias and R. Srivastava)

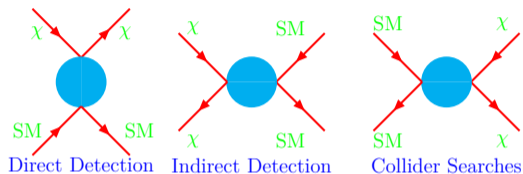
JCAP 03 (2024) 028

# Table of contents

- 1 Overview**
- 2 Introduction**
- 3 Dark matter landscape**
- 4 Thermal relic dark matter vs boosted dark matter**
- 5 DSNB boosted dark matter**
  - DSNB
  - Boosted dark matter flux at the underground detectors
  - Dark matter signal at the underground detectors
  - Resulting Limits
- 6 Conclusions**

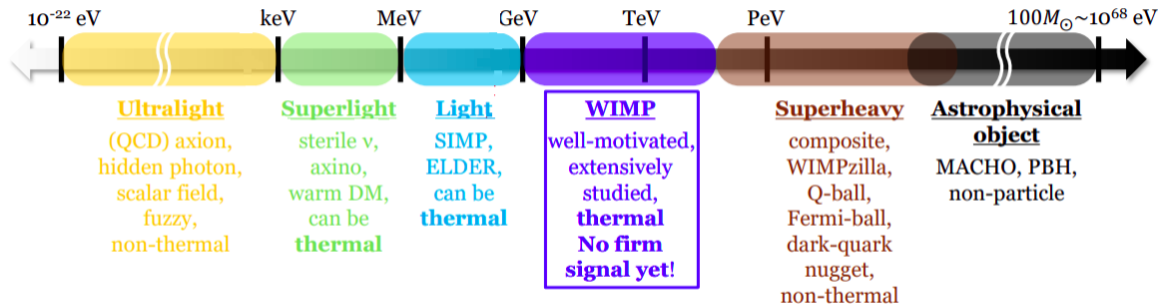
## Motivation for searching the Dark Matter (DM)

- Cold DM: It is a non-luminous matter which occupies 27% of the mass and energy in the observable Universe. It does not interact with photons and interacts only “weakly” with ordinary matter.
- Astronomical and cosmological observations at various scales:
  - (i) Rotation curves of spiral galaxies and galaxy clusters
  - (ii) Gravitational lensing
  - (iii) Cosmic Microwave background (CMB) fluctuations

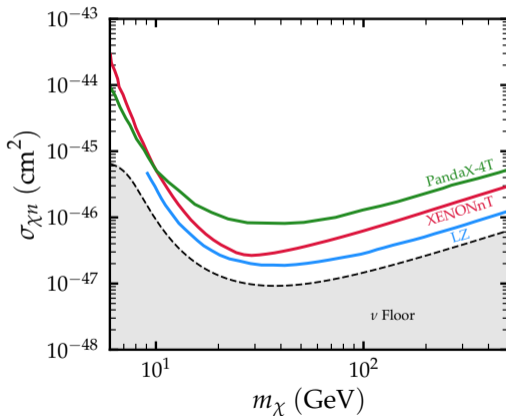
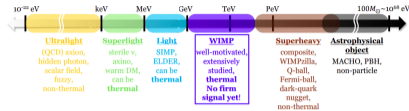


- **Direct Detection Experiments:** *XENONnT, LUX-ZEPLIN, Super-CDMS, Dark-Side, PandaX-4T, etc.*
- **Indirect Detection Experiment:** *IceCube, HESS, MAGIC, etc.*
- **Accelerator searches:** *ATLAS, CMS at CERN*

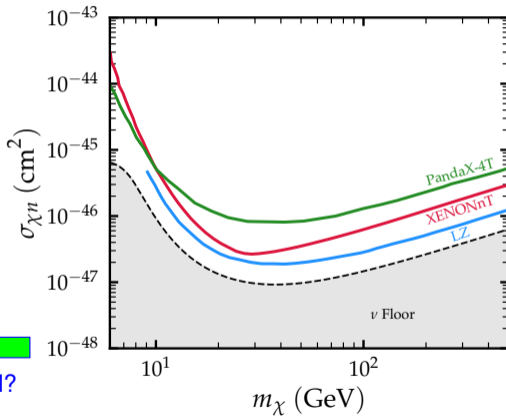
# DM landscape: a wide mass range



# DM landscape: a wide mass range



# DM landscape: a wide mass range



← light DM?

# Thermal relic DM vs boosted DM



The maximum recoil energy of the target:

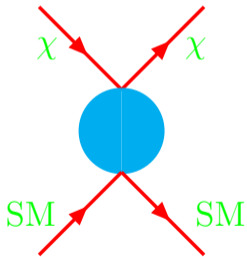
$$T_r^{\max} \approx \frac{Q^2}{2m_T} \approx \frac{2m_\chi^2 m_T v_\chi^2}{(m_\chi + m_T)^2}$$

# Thermal relic DM vs boosted DM



The maximum recoil energy of the target:

$$T_r^{\max} \approx \frac{Q^2}{2m_T} \approx \frac{2m_\chi^2 m_T v_\chi^2}{(m_\chi + m_T)^2}$$



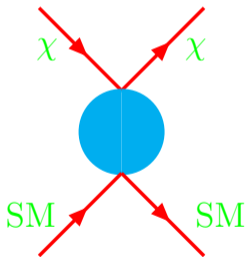
$$v_\chi \approx 10^{-3} c$$



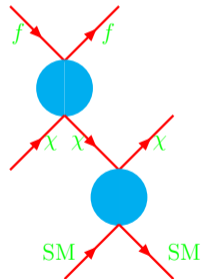
# Thermal relic DM vs boosted DM

The maximum recoil energy of the target:

$$T_r^{\max} \approx \frac{Q^2}{2m_T} \approx \frac{2m_\chi^2 m_T v_\chi^2}{(m_\chi + m_T)^2}$$



$$v_\chi \approx 10^{-3} c$$



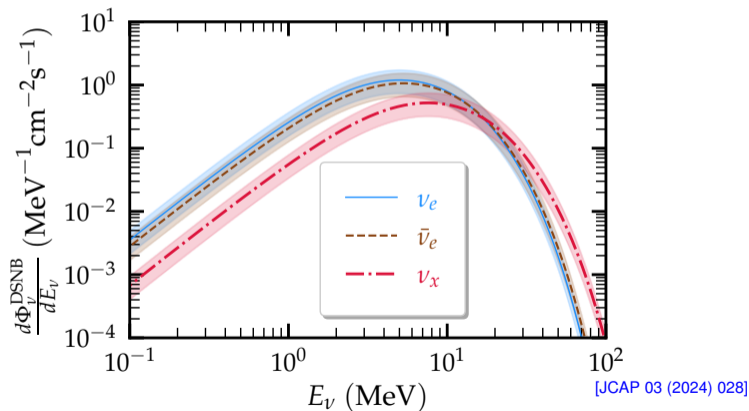
$$v_\chi \sim c$$

**DSNB boosted dark matter**

# Diffuse Supernova Neutrino Background



Right after the first star formation event, the Universe has been surrounded by an isotropic flux of MeV-energy neutrinos and antineutrinos of all flavors, produced from all supernovae events from the core-collapse explosions of huge stars throughout the Universe. This cumulative and isotropic flux of MeV neutrinos form DSNB.



The DSNB-boosted DM differential flux,

$$\frac{d\Phi_X}{dT_X} = D_{\text{halo}} \sum_{\alpha} \int_{E_{\nu}^{\text{min}}}^{E_{\nu}^{\text{max}}} dE_{\nu} \frac{1}{m_X} \frac{d\sigma_{\nu X}}{dT_X} \frac{d\Phi_{\nu\alpha}^{\text{DSNB}}}{dE_{\nu}}$$

- $D_{\text{halo}}$  encodes the line of sight integral of DM density within our galactic halo,

$$D_{\text{halo}} = \int_{\Delta\Omega} \frac{d\Omega}{4\pi} \int_0^{\ell_{\text{max}}} \rho_{\text{NFW}}[r(\ell, \psi)] d\ell$$

- We consider Navarro-Frenk-White (NFW) profile for galactic DM density,

$$\rho_{\text{NFW}}(r) = \rho_{\odot} \left[ \frac{r}{r_{\odot}} \right]^{-1} \left[ \frac{1 + \frac{r_{\odot}}{r_s}}{1 + \frac{r}{r_s}} \right]^2$$

- For the differential cross section, we assume the constant cross section approximation, i.e.

$$\frac{d\sigma_{\nu X}}{dT_X} = \frac{\sigma_{\nu X}}{T_X^{\text{max}}}$$

# BDM Flux At The Underground Detectors



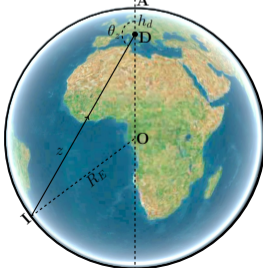
The DSNB-boosted DM differential flux,

$$\frac{d\Phi_\chi}{dT_\chi} = D_{\text{halo}} \sum_\alpha \int_{E_\nu^{\text{min}}}^{E_\nu^{\text{max}}} dE_\nu \frac{1}{m_\chi} \frac{d\sigma_{\nu\chi}}{dT_\chi} \frac{d\Phi_{\nu\alpha}^{\text{DSNB}}}{dE_\nu}$$

DM flux gets attenuated by the elements of the atmosphere and Earth before reaching to the underground detector. However as  $n_i^{\text{atm}} \ll n_i^{\text{Earth}}$ , we have **neglected the attenuation due to elements of the atmosphere.**

$$\frac{dT_\chi^z}{dz} = -n_i \int_0^{T_i^{\text{max}}(T_\chi^z)} \frac{d\sigma_{\chi i}}{dT_i} T_i dT_i$$

$$\frac{d\sigma_{\chi i}}{dT_i} = \frac{\sigma_{\chi i}}{T_i^{\text{max}}}$$
$$i \equiv \{e, \mathcal{N}\}$$



# BDM Flux At The Underground Detectors



The DSNB-boosted DM differential flux,

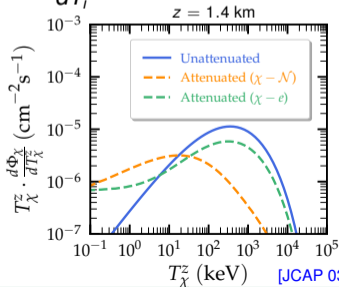
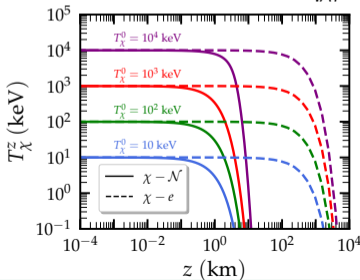
$$\frac{d\Phi_\chi}{dT_\chi} = D_{\text{halo}} \sum_\alpha \int_{E_\nu^{\text{min}}}^{E_\nu^{\text{max}}} dE_\nu \frac{1}{m_\chi} \frac{d\sigma_{\nu\chi}}{dT_\chi} \frac{d\Phi_{\nu\alpha}^{\text{DSNB}}}{dE_\nu}$$

DM flux gets attenuated by the elements of the atmosphere and Earth before reaching to the underground detector. However as  $n_i^{\text{atm}} \ll n_i^{\text{Earth}}$ , we have **neglected the attenuation due to elements of the atmosphere.**

$$\sigma_{\nu\chi} = \sigma_{\chi e} = \sigma_{\chi n} = 10^{-29} \text{ cm}^2$$

$$m_\chi = 300 \text{ MeV}$$

$$\frac{dT_\chi^z}{dz} = -n_i \int_0^{T_i^{\text{max}}(T_\chi^z)} \frac{d\sigma_{\chi i}}{dT_i} T_i dT_i$$



[JCAP 03 (2024) 028]

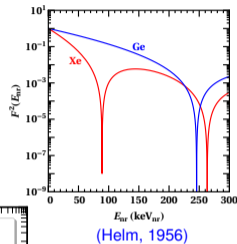
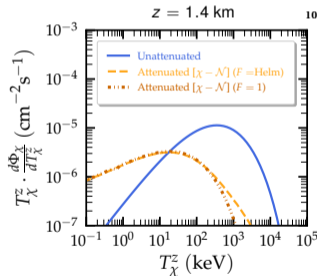
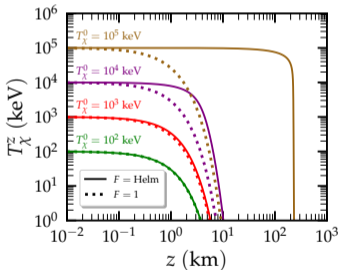
# Implications of nuclear form factor

The spin independent DM-nuclei scattering cross section can be written as,

$$\sigma_{\chi\mathcal{N}}^{\text{SI}}(q^2) = \frac{\mu_{\chi\mathcal{N}}^2}{\mu_{\chi n}^2} A^2 \sigma_{\chi n} F^2(q^2)$$

$$\sigma_{\chi\chi} = \sigma_{\chi e} = \sigma_{\chi n} = 10^{-29} \text{ cm}^2$$

$$m_{\chi} = 300 \text{ MeV}$$



[JCAP 03 (2024) 028]

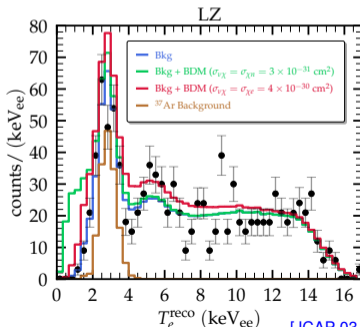
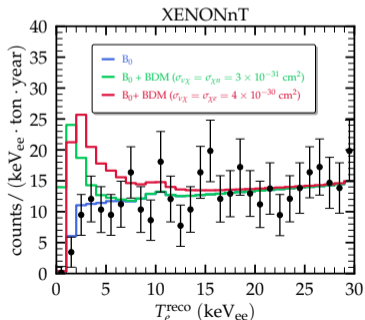
# DM signal at the underground detectors



After reaching the underground detector, the DSNB-boosted DM can scatter off both the electrons and nuclei of the target material, triggering both electronic and nuclear recoils. The differential event rate with respect to the recoil energy  $T_i$  can be written as,

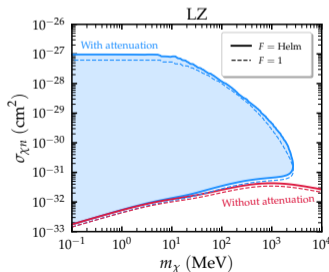
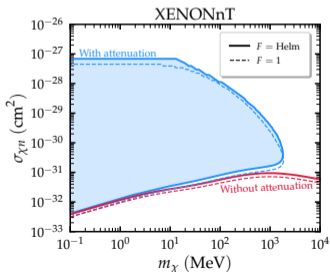
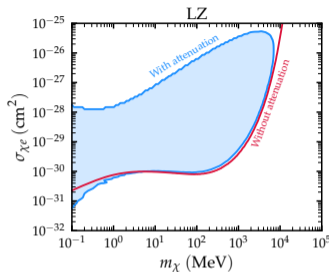
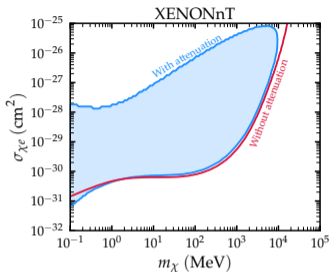
$$\frac{dR}{dT_i} = t_{\text{run}} N_{\text{target}}^i \mathcal{A} \int dT_{\chi}^z \frac{d\Phi_{\chi}}{dT_{\chi}^z} \frac{d\sigma_{\chi i}}{dT_i}$$

$$m_{\chi} = 300 \text{ MeV}$$

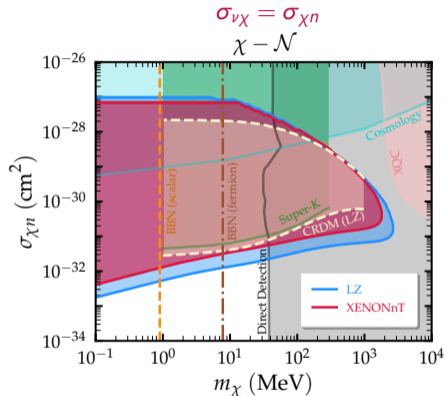
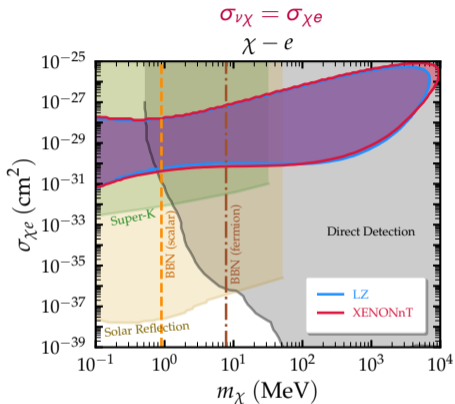




# Effect of Earth attenuation in the resulting limits



# Resulting Limits



V. De Romeri, A. Majumdar et al., JCAP 03 (2024) 028

# Conclusions

- DSNB Boosted DM produces a subdominant, semi-relativistic component of Galactic DM.
- Consideration of Earth attenuation is crucial for accurate interpretation of experimental results.
- *Although a significant part of our constraints lie in a region of parameter space already probed by other searches, these results highlight the complementarity and significance of the LZ and XENONnT data in probing the sub-GeV DM parameter space.*

THANK YOU

**Extras**

# $\chi^2$ function utilized

- For the analysis of LZ data, we have performed a spectral analysis using the following Poissonian  $\chi^2$  function

$$\chi^2(\vec{\mathcal{S}}; \alpha, \beta, \delta) = 2 \sum_{i=1}^{51} \left[ R_{\text{pred}}^i(\vec{\mathcal{S}}; \alpha, \beta, \delta) - R_{\text{exp}}^i + R_{\text{exp}}^i \ln \left( \frac{R_{\text{exp}}^i}{R_{\text{pred}}^i(\vec{\mathcal{S}}; \alpha, \beta, \delta)} \right) \right] + \left( \frac{\alpha}{\sigma_\alpha} \right)^2 + \left( \frac{\beta}{\sigma_\beta} \right)^2 + \left( \frac{\delta}{\sigma_\delta} \right)^2,$$

- The following Gaussian  $\chi^2$  function is used for the analysis of XENONnT data

$$\chi^2(\vec{\mathcal{S}}; \beta) = \sum_{i=1}^{30} \left( \frac{R_{\text{pred}}^i(\vec{\mathcal{S}}; \beta) - R_{\text{exp}}^i}{\sigma^i} \right)^2 + \left( \frac{\beta}{\sigma_\beta} \right)^2$$

# Geophysical properties of Earth

We model the Earth's interior as a sphere of constant electron and nuclear densities ( $n_e = 8 \times 10^{23} \text{ cm}^{-3}$  and  $n_N = 3.44 \times 10^{22} \text{ cm}^{-3}$ ), based on the abundances of the main elements as shown in following table.

Element	Mass Number (A)	Relative Abundance (%)	$n_N$ ( $\text{cm}^{-3}$ )
Fe	55.845	32.1	$6.11 \times 10^{22}$
O	15.999	30.1	$3.45 \times 10^{22}$
Si	28.086	15.1	$1.77 \times 10^{22}$
Mg	24.305	13.9	$1.17 \times 10^{22}$
S	32.065	2.9	$2.33 \times 10^{21}$
Ca	40.078	1.5	$7.94 \times 10^{20}$
Al	26.982	1.4	$1.09 \times 10^{21}$